Regular Article

PHYSICAL CHEMISTRY RESEARCH
Published by the
Iranian Chemical Society
www.physchemres.org
info@physchemres.org

***Phys. Chem. Res.**, Vol. 5, No. 1, 99-112, March 2017*
DOI: 10.22036/pcr.2017.38496

Variational Calculations for the Relativistic Interacting Fermion System at Finite Temperature: Application to Liquid ^{3}He

G.H. Bordbar*, S. Mizani and M.T. Mohammadi Sabet

Physics Department, Shiraz University, Shiraz 71454, Iran

(Received 21 March 2016, Accepted 17 October 2016)

In this paper, at first we formulate the lowest order constrained variational method for the relativistic case of an interacting fermion system at finite temperature. Then, we used this formalism to calculate some thermodynamic properties of liquid ^{3}He in the relativistic regime. The results show that the difference between total energies of the relativistic and non-relativistic cases of liquid ^{3}He decreases by increasing the density. On the other hand, at densities smaller than $\rho = 0.010$ Å^{-3}, which is close to the theoretical saturation point of the system, this difference increases as the temperature increases. We also found that the relativistic calculations lead to the thermodynamic characteristics for liquid ^{3}He which are in a better agreement with the experimental data with respect to those of non-relativistic calculations.

Keywords: Liquid ^{3}He, Thermodynamic properties, Lowest order constrained method, Relativistic corrections, Cluster expansion

INTRODUCTION

Liquid ^{3}He, an important system in the condensed matter physics, is the only real fermionic fluid which has unique properties [1,2]. To investigate this system theoretically, the most important theory is the Landau phenomenological theory which introduces the quasiparticles concept [3,4]. Although this theory provides accurate description of the observed experimental properties of liquid ^{3}He, it has some shortcomings, *e.g.*, due to the finite lifetime of quasiparticles, they are well-defined only at low temperatures and because of the many-particle nature of liquid ^{3}He, the Landau parameters are undetermined in this theory [5]. Therefore, different many-body methods have been employed to investigate the properties of liquid ^{3}He. These methods include Monte Carlo-Green function which determines the ground state energy of the liquid ^{3}He [6], the Fermi-hypernated chain which is a variational method [7], the correlated basis functions which contain a perturbation term of strong repulsive force in the potential [8,9] and the density functional theory based on the variation of energy with respect to density [10,11]. Despite all made efforts, there is no comprehensive microscopic theory to describe the behavior of liquid ^{3}He exactly and all performed works have the relative and partial agreement with the experimental results. In majority of the mentioned many-body methods, the trial wave function of the *N*-body system is considered as multiplication of the Slater determinant of *N* non-interacting particles and the correlation operator. Therefore, in order to obtain the better results and a more accurate microscopic method including all properties of liquid ^{3}He, some corrections have been made in the correlation operator. These corrections include backflow effects [12], momentum dependency in the correlations [13] and spin-spin correlations [14-16]. In spite of these corrections, the results of microscopic methods do not show a good agreement with the experimental results.

On the other hand, one important issue in highly correlated fermionic systems is the investigation of relativistic effects on the properties of these systems. The relativistic effects play an important role in nuclear matter [17,18], electron gas [19-20], and chemical systems [21,22].

*Corresponding author. E-mail: ghbordbar@shirazu.ac.ir

Considering the relativistic form of energy plays also an important role in the properties of fermionic systems in different phases and the pairing mechanism of these systems [23]. Therefore, knowing the properties of a relativistic fermionic systems can help to get some insights into these up-to-now underlying issues. Special characteristic of liquid ^{3}He as the only real fermionic system motivated us to study its properties using a variational method.

Lowest order constrained variational (LOCV) method, adopted in this paper, is one of the microscopic methods to investigate the highly correlated systems. This method, which is based on the cluster expansion of energy functional, is a self-consistent method and does not generate any free parameter. We have investigated the thermodynamic properties of liquid ^{3}He using this method. The results obtained by this method have a good agreement with experimental results [14-16].

Another motivation for considering the relativistic ^{3}He is that in real cases the energy of a particle obeys special theory of relativity. Therefore, unlike the other techniques in which correlation function is employed to improve the systems, we count on the energy of the ^{3}He atoms in a relativistic regime. Therefore, In fact, in this paper we use the LOCV method and investigate the thermodynamic properties of liquid ^{3}He considering the relativistic form of the energy. In other words, the effects of relativistic correction have been investigated to test the obtained results. Some theoretical discussions and some comparisons will be included to provide new insights into this system.

RELATIVISTIC LOCV FORMALISM

The lowest order constrained variational method is based on cluster expansion of energy functional [24],

$$E = \frac{1}{N}\frac{\langle \Psi | H | \Psi \rangle}{\langle \Psi | \Psi \rangle} = E_1 + E_2 + \ldots \tag{1}$$

where E_1 and E_2 are respectively one-body energy per particle and the two-body energy per particle, *etc.*

Now, we consider a system of N interacting atoms. The number of particles of this system is,

$$N = \sum_{k\sigma} n(k) \tag{2}$$

where n(k) is the Fermi-Dirac distribution function,

$$n(k) = \frac{1}{\exp((\varepsilon(\mathrm{k}) - \mu)/\mathrm{K}_B T) + 1} \tag{3}$$

In Eq. (3), ε(k) is the single particle energy which in the relativistic form is,

$$\varepsilon(\mathrm{k}) = \sqrt{\hbar^2 c^2 k^2 + m^2 c^4} - mc^2 \tag{4}$$

and in the case of non-relativistic is,

$$\varepsilon(\mathrm{k}) = \frac{\hbar^2 k^2}{2m} \tag{5}$$

In the above equations μ is the chemical potential obtained by considering the following constraint,

$$\begin{aligned} N &= \sum_{k\sigma} n(k) = \frac{\upsilon\Omega}{(2\pi)^3}\int d^3 k n(k) \\ \Rightarrow \rho &= \frac{\upsilon}{2\pi^2}\int_0^\infty \frac{\mathrm{k}^2 \mathrm{dk}}{e^{\beta(\sqrt{\hbar^2 c^2 k^2 + m^2 c^4} - mc^2 - \mu)} + 1} \end{aligned} \tag{6}$$

In the cluster expansion method, the one-body energy per particle at finite temperature is as follows,

$$E_1 = \frac{1}{N}\sum_{k\sigma} \varepsilon(\mathrm{k}) n(\mathrm{k}) \tag{7}$$

Therefore, after some algebra we have the following relations for the one-body energy per particle at finite temperature,

$$E_1 = \begin{cases} \dfrac{\upsilon}{2\pi^2\rho}\displaystyle\int_0^\infty \frac{(\frac{\hbar^2}{2m})}{e^{\beta(\frac{\hbar^2 k^2}{2m} - \mu)} + 1}\mathrm{k}^4 \mathrm{dk}; & Non-Relativistic \\ \dfrac{\upsilon}{2\pi^2\rho}\displaystyle\int_0^\infty \frac{(\sqrt{\hbar^2 c^2 k^2 + m^2 c^4} - mc^2)}{e^{\beta(\sqrt{\hbar^2 c^2 k^2 + m^2 c^4} - mc^2 - \mu)} + 1}\mathrm{k}^2 \mathrm{dk}; & Relativistic \end{cases} \tag{8}$$

For the two-body energy per particle we have [24],

$$E_2 = \frac{1}{2N}\sum_{ij}\langle ij\,|\,\mathrm{W}(12)|\,ij\,\rangle_a \tag{9}$$

In the above equation, W (12) is the effective two-body potential,

$$\mathrm{W}(12) = \frac{1}{2}F^{\dagger}(12)\big[t(1)+t(2),\mathrm{F}(12)\big]+\frac{1}{2}\big[F^{\dagger}(12),t(1)+t(2)\big]F(12)+F^{\dagger}(12)\,\mathrm{V}(12)\,\mathrm{F}(12) \tag{10}$$

where F (12) is the two-body correlation operator, V (12) is the two-body potential and $t(i)$ is the kinetic energy operator which we consider it in the relativistic form.

After doing some algebra, we get the following relation for the two-body effective potential in the relativistic regime,

$$W(12) = W_{NR}(12)+W_{R1}(12)+W_{R2}(12) \tag{11}$$

where W_{NR} (12) is the effective two-body potential of non-relativistic ^{3}He and W_{R1} (12) and W_{R2} (12) are the first and second order relativistic corrections in the effective two-body potential of liquid ^{3}He, respectively.

$$\begin{aligned}
W_{NR}(12) &= \frac{\hbar^2}{m}(\nabla F(r))^2 + F^2(\mathrm{r})\,\mathrm{V}(\mathrm{r})\\
W_{R1}(12) &= \frac{\hbar^4}{8m^3c^2}\left\{8\nabla F(r).\nabla^3 F(r)+6\nabla^2 F(r)\nabla^2 F(r)\right\}\\
W_{R2}(12) &= \frac{\hbar^6}{16m^5c^4}\left\{30\nabla^2 F(r)\nabla^4 F(r)+12\nabla F(r).\nabla^5 F(r)+20\nabla^3 F(r).\nabla^3 F(r)\right\}
\end{aligned} \tag{12}$$

In Eq. (12), $V(r)$ is the inter-particle potential used as the Lennard-Jones potential, and $f(r)$ is the two-body correlation function. After some algebra, the following equation is obtained for the relativistic two-body energy per particle,

$$E_2 = 2\pi\rho\int_0^{\infty}\left(1-\frac{1}{2\rho^2}\big[\gamma(r)\big]^2\right)r^2 dr\,\big[W(\mathrm{r})\big] \tag{13}$$

where $\gamma(r)$ is as follows,

$$\gamma(r) = \frac{1}{\pi^2}\int_0^{\infty}\frac{\sin kr}{kr}n(\mathrm{k})\,\mathrm{k}^2\,dk \tag{14}$$

We can write Eq. (13) as,

$$E_2 = E_2^{NR} + 2\pi\rho\int_0^{\infty}\left(1-\frac{1}{2\rho^2}\big[\gamma(r)\big]^2\right)r^2 dr\,\big[W_{R1}(\mathrm{r})+W_{R2}(\mathrm{r})\big] \tag{15}$$

where the first term, E_2^{NR}, is the non-relativistic two-body energy per particle, and the second term is due to the relativistic corrections in the two-body energy. The non-relativistic two-body energy, E_2^{NR} is as follows,

$$E_2^{NR} = 2\pi\rho\int_0^{\infty}\left(1-\frac{1}{2\rho^2}\big[\gamma(r)\big]^2\right)r^2 dr\,\big[W_{NR}(\mathrm{r})\big] \tag{16}$$

To obtain the thermodynamic properties of the system, relation,

$$F = E - TS \tag{17}$$

where E is the total energy, T is the temperature and S is the entropy which for N fermion is as follows [25],

$$S = -k_B\sum_{\varepsilon}\{\ \langle 1-n(\varepsilon)\rangle\ln\langle 1-n(\varepsilon)\rangle+\langle n(\varepsilon)\rangle\ln\langle n(\varepsilon)\rangle\ \} \tag{18}$$

Now, we minimize the free energy with respect to the variation in the correlation function, $f(r)$, under the normalization constraint [26],

$$\sum_{ij}\langle ij\,|f^{\,2}(r)-f_p^{\,2}(\mathrm{r})|\,ij\,\rangle_a = 0 \tag{19}$$

where

$$F_P(\mathrm{r}) = \left[1-\frac{1}{2\rho^2}\big(\gamma(r)\big)^2\right]^{\frac{-1}{2}} = \big[a^2(r)\big]^{\frac{-1}{2}} \tag{20}$$

By this minimization, we get the following differential equation for the two-body correlation function

$$g''(r)-\left\{\frac{a''(r)}{a(r)}+\frac{m}{\hbar^2}(\mathrm{V}(\mathrm{r})+\lambda)\right\}g(r) = 0 \tag{13}\ (21)$$

where $g(r) = f(r)\ a(r)$ and λ is the Lagrange multiplier imposed by the normalization constraint. The two-body

correlation function is obtained by solving this differential equation numerically, and then the energy of the system can be calculated.

RESULTS AND DISCUSSION

In this section, we present the results of our calculations for the thermodynamic properties of liquid ^{3}He in the relativistic regime, and compare the results with those of non-relativistic case and also the experimental data.

As the first theoretical investigation of the relativistic effects, we investigate the kinetic energy of liquid ^{3}He. In Fig. 1, the kinetic energy per particle (one-body energy) of liquid ^{3}He is shown as a function of density at different temperatures, in the relativistic and non-relativistic cases. This figure shows that at a given temperature, for densities smaller than about ρ = 0.014 Å^{-3}, the kinetic energy of relativistic liquid ^{3}He is smaller than that of non-relativistic case and their differences are considerable especially at $T \gtrsim$ 0.5 *K*. At this density range, the relativistic curves have more difference with the non-relativistic system by increasing the temperature and decreasing the density as well. As we documented previously [15-16], the saturation point of these system, *i.e.* the minimum point of total energy, occurs at ρ = 0.012 Å^{-3}, and the density ρ = 0.014 Å^{-3} is very close to the saturation point. Saturation point is a density in which the helium droplets begin to construct. Therefore, at the densities smaller than this point, the system tends to be more gaseous. The energy and momentum of this system at these densities can be considered nonrelativistic. On the other hand, calculations of partition function [20] show that in both quantum and classical systems, the relativistic effects lead to the increase of the kinetic energy, and by increasing the temperature, the portion of interaction becomes less influencing and the difference between relativistic and non-relativistic systems increases. In other words, the main difference between relativistic and non-relativistic systems lies in the kinetic energy contribution. This is the main reason for more difference in the kinetic energies of relativistic and non-relativistic cases at high temperature. Figure 1 also shows that the relativistic and non-relativistic results are nearly similar for densities greater than ρ = 0.014 Å^{-3} at temperatures smaller than T = 1.5 *K*. At these densities, the difference in kinetic energies of relativistic and non-relativistic liquid ^{3}He decreases by increasing the temperatures. On the other hand, at temperatures in the range of 2.5 $K \lesssim T \lesssim$ 3.5 *K*, for densities greater than ρ = 0.014 Å^{-3}, the kinetic energy of relativistic liquid ^{3}He is greater than that of non-relativistic case.

The results of two-body energy per particle for relativistic and non-relativistic liquid ^{3}He are compared for different densities in Tables 1 and 2 at T = 1.5 and T = 2.5 *K*, respectively. In these tables, E_2^{NR} (E_{2R}) denotes for non-relativistic (relativistic) two-body energy per particle of liquid ^{3}He. As mentioned previously, the relativistic two-body energy per particle consists of three parts (see Eq. (15)). At a given temperature, the effect of this corrections is of the order of 10^{-3} and for some densities it reaches to the order of 10^{-2}. It was found that as the temperature increases, the magnitude of the relativistic corrections in the two-body energy of liquid ^{3}He increases up to 10^{-1}. However, by increasing the density, generally, the effect of this corrections reaches to the order of 10^{-3} and for some densities to the order of 10^{-1}. Our results show that in most densities, for the relativistic liquid ^{3}He, the two-body energy per particle is smaller than that for the non-relativistic case. The importance of these results is that considering the relativistic form for the energy of fermions affects the two-body correlation function and therefore the portion of effective potential (see Eqs. (11) and (12)). Therefore, the interaction energy of the system, E_2, also changes.

In Fig. 2, the total energies per particle of relativistic and non-relativistic liquid ^{3}He at different temperatures are plotted versus density. This figure shows that the total energies of relativistic and non-relativistic liquid ^{3}He have a considerable difference for $\rho \lesssim$ 0.010 Å^{-3} which is close to the saturation point. This difference increases by increasing the temperature, but both systems behave similar for ρ $\rho \gtrsim$ 0.010 Å^{-3}. By increasing the temperature, this difference is very small at densities greater than about 0.010 Å^{-3} except for temperature range 0.5 $K \lesssim T <$ 1.5 *K* in which the difference is approximately constant as the density increases up to ρ = 0.017 Å^{-3}. As clearly shown in Fig. 2, for $\rho \gtrsim$ 0.010 Å^{-3}, the behavior of total energy curve of relativistic liquid ^{3}He at temperature range 1.5 $K \lesssim T \lesssim$ 2.5 *K*, is not similar with other temperature ranges. At this temperature range, unlike $T \lesssim$ 1.5 *K*, for densities greater

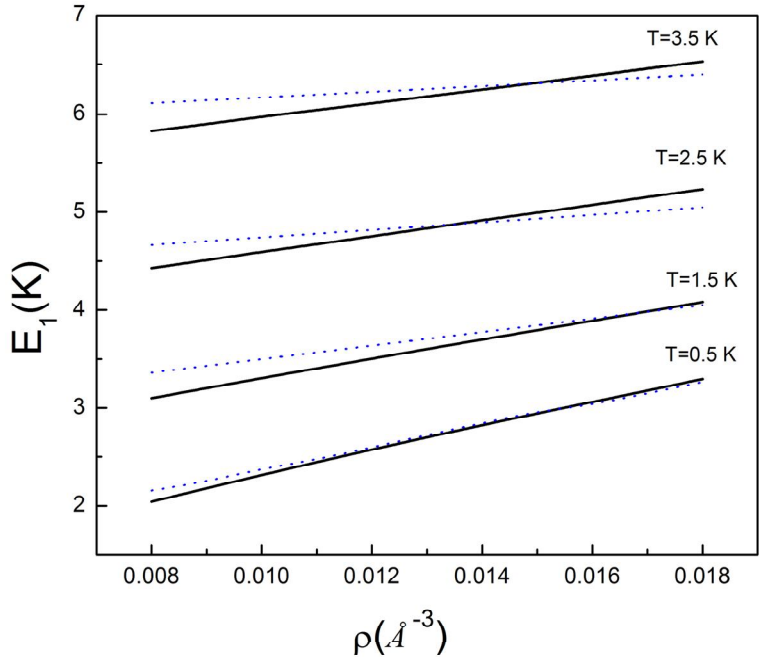

Fig. 1. One-body (kinetic) energy per particle of liquid ^{3}He as a function of density at different temperatures. Dotted (full) curves show the none-relativistic (relativistic) total energy.

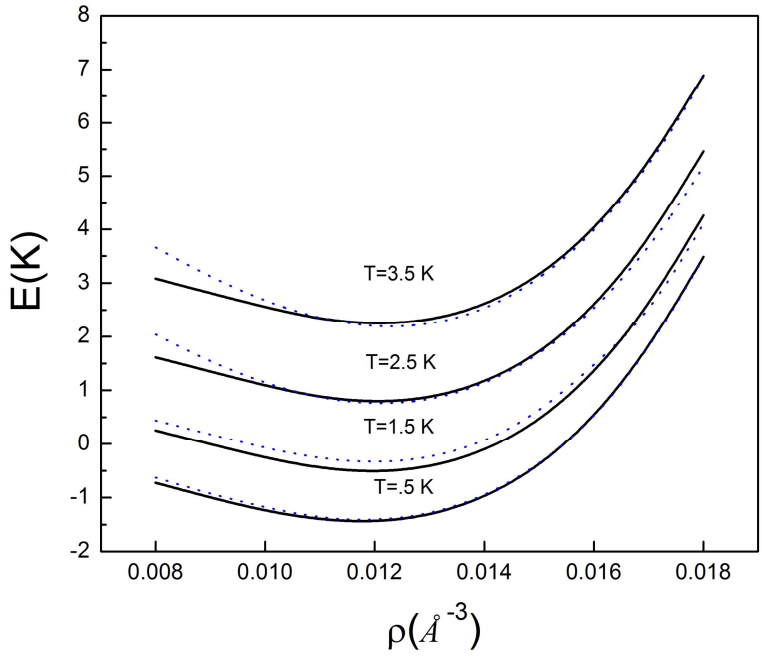

Fig. 2. Total energy per particle of liquid ^{3}He as a function of density at different temperatures. Dotted (full) curves show the none-relativistic (relativistic) total energy.

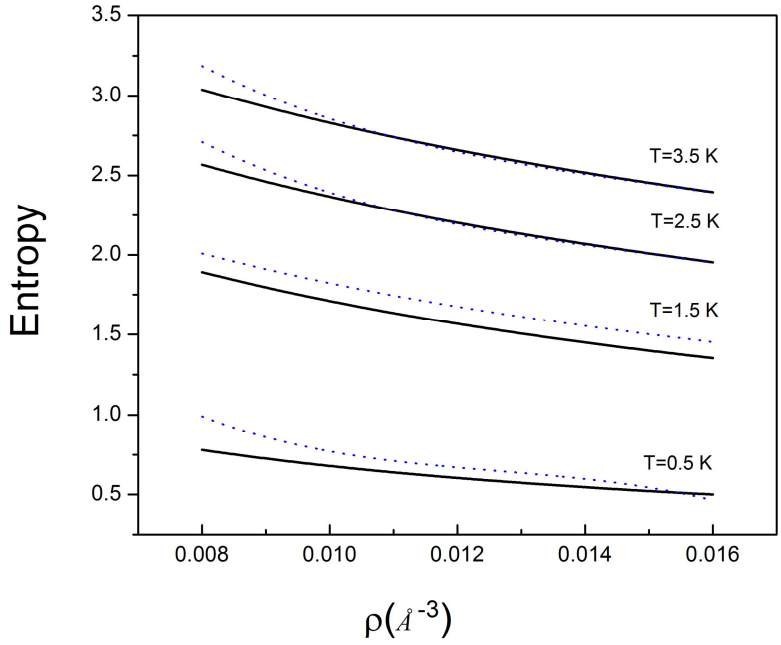

Fig. 3. The entropy as a function of density for the relativistic liquid ^{3}He (full curves) and for non-relativistic liquid ^{3}He (dotted curves) at different temperatures.

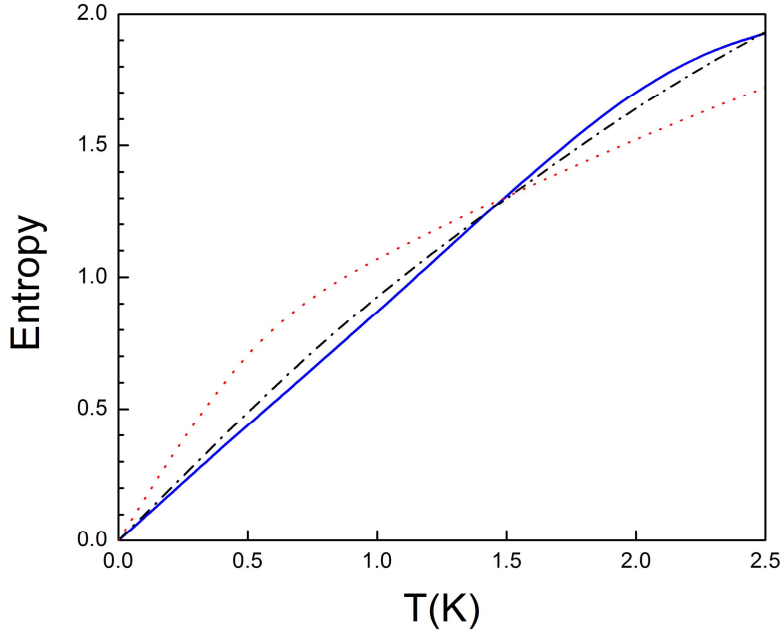

Fig. 4. The entropy as a function of temperature for the relativistic liquid ^{3}He (dash-dotted curve) and non-relativistic liquid ^{3}He (full curve) at ρ = 0.0164 Å^{-3}. Dotted curve shows the experimental results [23].

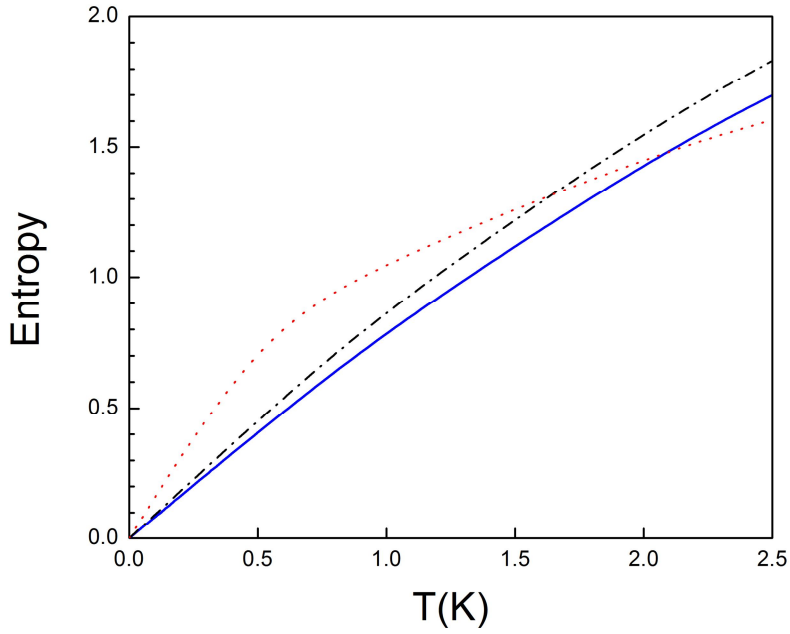

Fig. 5. The entropy as a function of temperature for the relativistic liquid ^{3}He (dash-dotted curve) and non-relativistic liquid ^{3}He (full curve) at $\rho = 0.0185$ Å^{-3}. Dotted curve shows the experimental results [23].

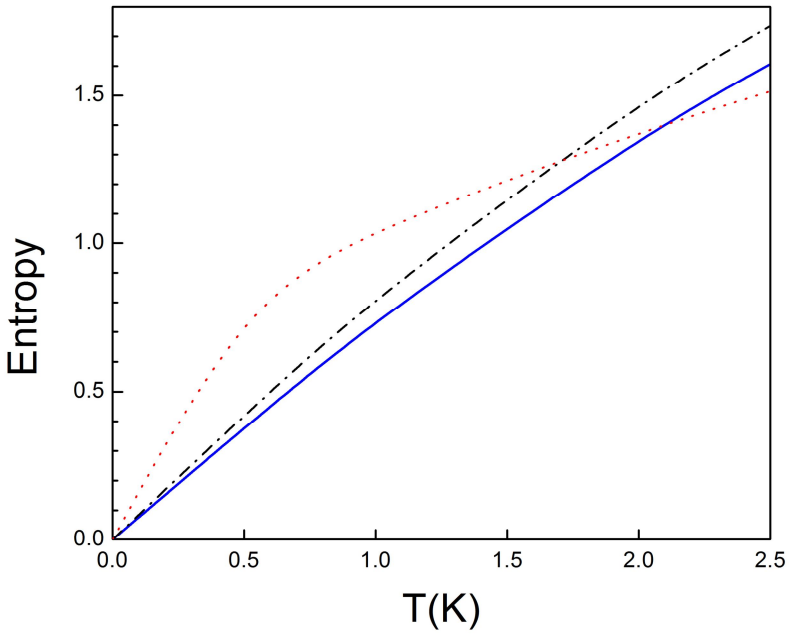

Fig. 6. The entropy as a function of temperature for the relativistic liquid ^{3}He (dash-dotted curve) and non-relativistic liquid ^{3}He (full curve) at $\rho = 0.0208$ Å^{-3}. Dotted curve shows the experimental results [23].

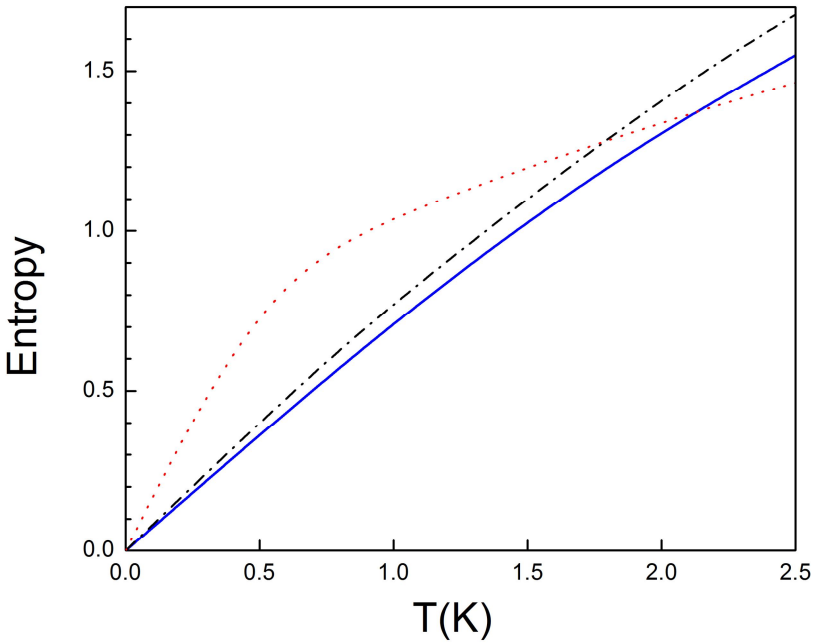

Fig. 7. The entropy as a function of temperature for the relativistic liquid ^{3}He (dash-dotted curve) and non-relativistic liquid ^{3}He (full curve) at $\rho = 0.0224$ Å^{-3}. Dotted curve shows the experimental results [23].

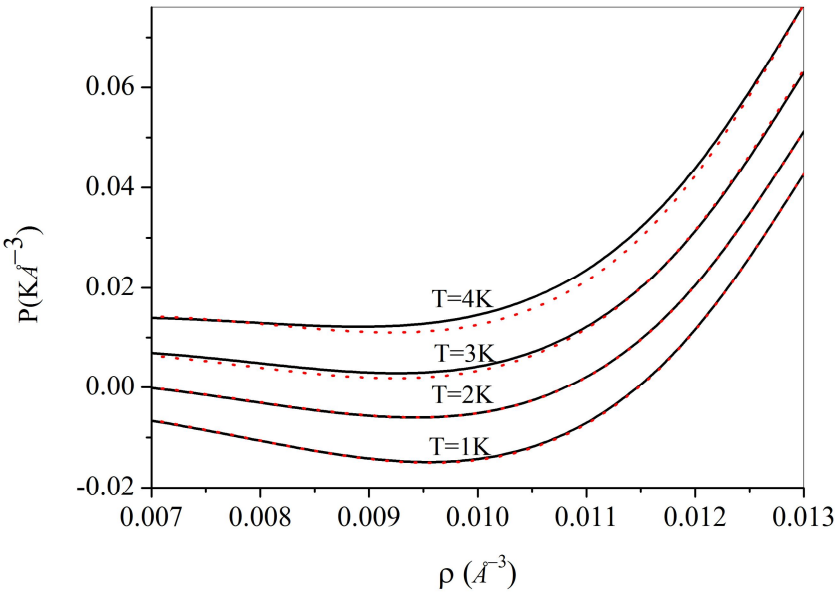

Fig. 8. The pressure of relativistic (full curves) and non-relativistic liquid ^{3}He (dotted curves) as a function of density for different temperatures.

Table 1. The Comparison of Two-body Energy per Particle for Relativistic and Non-relativistic Liquid ^{3}He at $T = 1.5\ K$

ρ (Å^{-3})	E_{2NR} (K)	E_{2R} (K)
0.008	-2.8469	-2.8492
0.009	-3.2036	-3.2078
0.01	-3.5580	-3.5650
0.011	-3.8522	-3.8602
0.012	-4.0284	-4.0360
0.013	-4.0357	-4.0437
0.014	-3.8328	-3.8414
0.015	-3.3691	-3.3774
0.016	-2.5790	-2.5880
0.017	-1.4218	-1.4204
0.018	0.1817	0.1774

Table 2. The Comparison of Two-body Energy Per particle for Relativistic and Non-relativistic Liquid ^{3}He at $T = 2.5\ K$

ρ (Å^{-3})	E_{2NR} (K)	E_{2R} (K)
0.008	-2.7954	-2.8131
0.009	-3.1408	-3.1608
0.010	-3.5053	-3.5082
0.011	-3.8025	-3.8052
0.012	-3.9755	-3.9781
0.013	-3.9830	-3.9870
0.014	-3.7803	-3.7843
0.015	-3.3172	-3.3206
0.016	-2.5285	-2.5324
0.017	-1.3630	-1.3680
0.018	0.2130	0.2287

Table 3. The Comparison of Free Energy for Relativistic and Non-relativistic Liquid ^{3}He with the Experimental Results at $\rho = 0.0166$ Å^{-3}

T (K)	E_{NR} (K)	F_R (K)	F_{EXP} (K)
0.5	0.96095	0.95944	0.796300
1	0.59531	0.58864	0.425930
1.5	0.02321	0.02038	-0.203704
2	-0.68239	-0.70772	0.833333

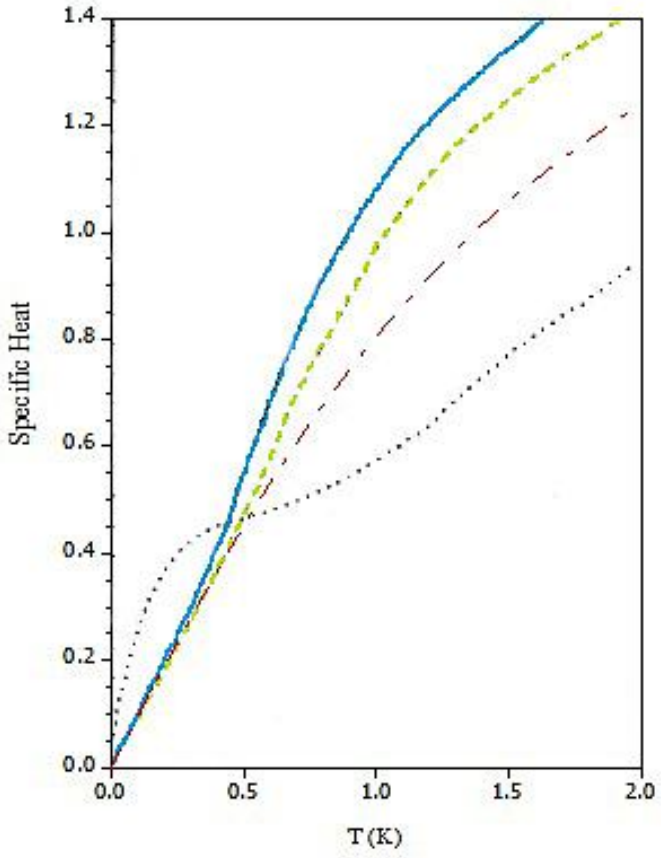

Fig. 9. The specific heat *vs.* temperature for relativistic (dash-dotted curve) and non-relativistic (full curve) liquid ^{3}He for $\rho = 0.0166$ Å^{-3}. The results of FPS calculations [24] (dashed-curves) and the experimental data[2] (Dotted curve) are also shown for comparison.

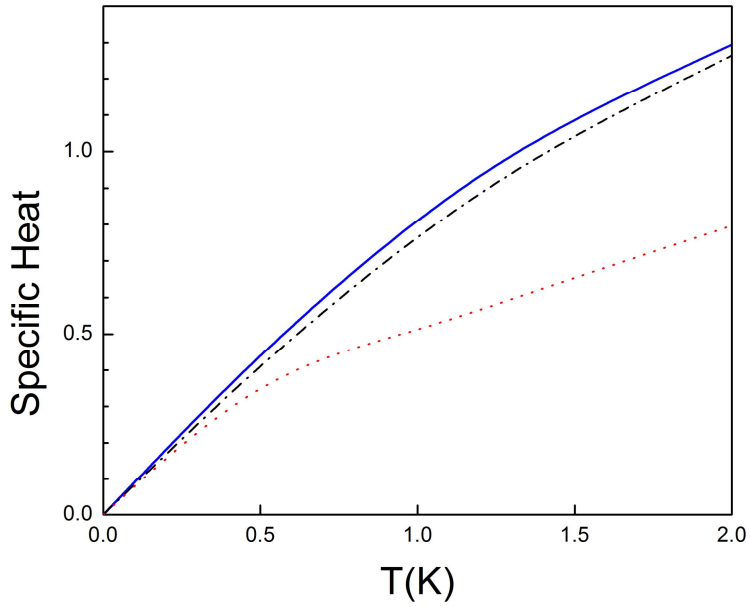

Fig. 10. The specific heat *vs*. temperature for relativistic (dash-dotted curve) and non-relativistic (full curve) liquid ^{3}He for $\rho = 0.0164$ Å^{-3}. The results of FPS calculations [24] (dashed-curves) and the experimental data [2] (Dotted curve) are also shown for comparison.

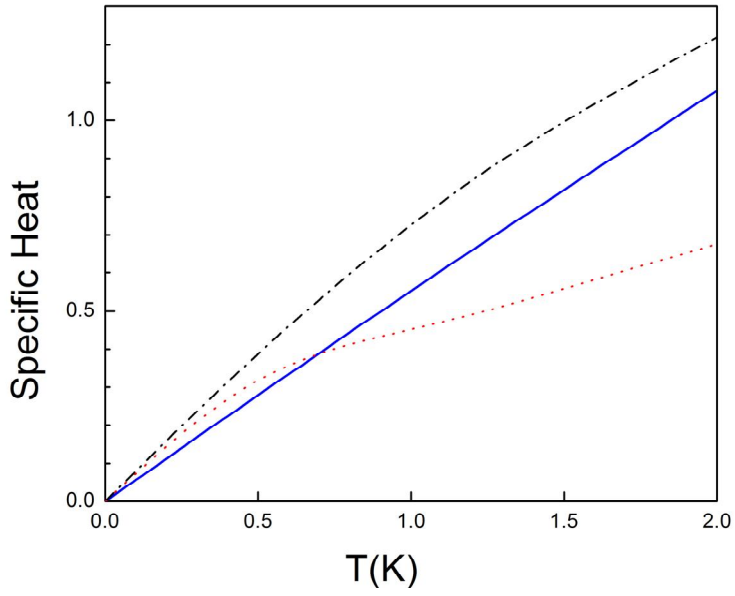

Fig. 11. The specific heat *vs*. temperature for relativistic liquid ^{3}He (dash-dotted curve) and non-relativistic liquid ^{3}He (full curve) at $\rho = 0.0185$ Å^{-3}. Dotted curve shows the experimental results [23].

than 0.017 Å^{-3}, the total energy of relativistic liquid ^{3}He is greater than that of non-relativistic case. Since the total energy of the system is the sum of one-body and two-body energies, it is concluded that the dominant term of energy is the one-body energy. Here, it should be noted that these density and temperature dependences of total energy are mainly due to the behavior of kinetic energy contribution which was given in the previous discussions regarding the kinetic energy of this system (Fig. 1).

Now, for further investigation, our calculations will be compared with some experimental data. In Fig. 3, the entropy at different temperatures is plotted as a function of density. At $T \lesssim 1.5$ *K*, for all densities, the entropy of relativistic liquid ^{3}He is smaller than that of non-relativistic case, and their difference decreases by increasing the density. On the other hand, this behavior is not seen at $T \gtrsim 1.5$. Especially at $T \gtrsim 2$ *K*, for densities greater than about 0.010 Å^{-3}, the entropy of non-relativistic liquid ^{3}He is smaller than that of relativistic liquid case. We can see that by increasing temperature, the difference between entropies of these cases decreases for $\rho \lesssim 0.010$ Å^{-3}. We found that this behavior is not observed at 1.5 $K \lesssim T \lesssim 2$ *K*, and in this range, the difference of entropies of relativistic and non-relativistic liquid ^{3}He is almost constant for all densities. Figure 4 shows the entropy of the system as a function of temperature at $\rho = 0.0164$ Å^{-3} for both relativistic and non-relativistic liquid ^{3}He. The experimental data [27] are also plotted for comparison. As seen in this figure, the entropy of relativistic system becomes closer to that of experiment. This behavior is held nearly for all considered temperatures. The entropy of system as a function of temperature for $\rho = 0.0185$ Å^{-3} is plotted in Fig. 5. The experimental results are also presented for comparison. At $T \lesssim 1.7$ *K*, the results of relativistic liquid ^{3}He are closer to experimental data with respect to the non-relativistic case, however at temperatures greater than about this temperature, the non-relativistic results are better. Figures 6 and 7 show the entropy of system for densities $\rho = 0.0208$ Å^{-3} and $\rho = 0.0224$ Å^{-3}, respectively. For $\rho = 0.0208$ Å^{-3}, at $T \lesssim 1.75$ *K*, the entropy difference between the relativistic system and experimental data is smaller than that of the non-relativistic liquid ^{3}He. This behavior is also observed for $\rho = 0.0224$ Å^{-3} at $T \lesssim 1.8$ *K*.

In Table 3, the free energies of relativistic and non-relativistic liquid ^{3}He and the experimental data [27] are compared for $\rho = 0.0166$ Å^{-3}. As it is seen, at all temperatures, the free energy of relativistic liquid ^{3}He has a more agreement with experimental data with respect to the non-relativistic case. This indicates that is preferred to consider the liquid ^{3}He as a relativistic system at $T \gtrsim 2$ *K*. It is found that at these temperatures, the magnitude of relativistic corrections is of the order of 0.01 *K* which is relatively large.

The pressure of relativistic liquid ^{3}He has been plotted as a function of density for some temperatures. This figure shows that by increasing the temperature, the equation of state of liquid ^{3}He becomes more stiffer, and therefore the system becomes more incompressible. From the equation of state, the critical temperature, at which the phase transition between vapor and liquid occurs, can be obtained using the inflection point condition of $(P - \rho)$-isotherms,

$$\left(\frac{\partial P}{\partial \rho}\right)_{T=T_C} = 0 \qquad \left(\frac{\partial^2 P}{\partial \rho^2}\right)_{T=T_C} = 0 \tag{22}$$

Our results show that the value of critical temperature is 4.5 *K* (4.8 *K*) for relativistic (non-relativistic) liquid ^{3}He. Experimental critical temperature is 3.32 *K* [29]. This shows that considering the liquid ^{3}He as a relativistic system leads to a considerable effect on the critical temperature, and the relativistic corrections are relatively important.

The specific heat of relativistic and non-relativistic liquid ^{3}He as well as the results of *FPS* [28] and experimental data are shown in Fig. 9. As shown in this figure, although, our results of both relativistic and non-relativistic liquid ^{3}He have a good agreement with *FPS* data, the specific heat of relativistic case shows a better agreement. At 0.5 $K \lesssim T \lesssim 2$ *K*, our results for relativistic liquid ^{3}He become closer to experimental data rather than *FPS* data and the results of non-relativistic liquid ^{3}He. The specific heat as a function of temperature is plotted for densities $\rho = 0.0164$ and 0.0185 Å^{-3} in Figs. 10 and 11, respectively. The experimental data [23] are also shown for comparison. Our results show that the specific heat of relativistic liquid ^{3}He becomes close to experimental data at $T \lesssim 0.5$ *K*. Furthermore, for $\rho = 0.0164$ Å^{-3}, the difference

between specific heat of relativistic liquid ^{3}He and experimental data is smaller than that of non-relativistic case.

SUMMARY AND CONCLUSIONS

In this work, the lowest order constrained variational method was formulated for an interacting fermion system in the relativistic case, then some thermodynamic properties of liquid^{3}He in the relativistic regime were calculated at finite temperature using this formalism. The Lenard-Jones potential was used in our calculations. The calculated properties of this relativistic system were compared with those of the non-relativistic case and also were compared with the experimental results. Our results showed that the kinetic energy (one-body energy per particle) of relativistic and non-relativistic liquid ^{3}He increases with increasing temperature and density as well. It was found that in most densities, the two-body energy per particle for the relativistic liquid ^{3}He is less than that for the non-relativistic case. It was found that in the term of total energy which is the sum of one-body and two-body energies, the dominant term is the one-body energy. Our calculations showed that the entropy of relativistic and non-relativistic liquid ^{3}He increases by decreasing the temperature and increasing density. We also found that the free energy of relativistic case of the system is closer to the experimental values with respect to the non-relativistic case. This behavior is more obvious at temperatures greater than $T = 2$ *K*. The difference between specific heat of relativistic liquid ^{3}He and experimental data is smaller than that of non-relativistic case and experimental data. The pressure curve of relativistic liquid ^{3}He showed that the equation of state of liquid ^{3}He becomes stiffer, and therefore the system is more incompressible by increasing the temperature. The critical temperature of non-relativistic liquid ^{3}He is $T_C = 4.8$ *K*, $T_C = 4.8$ *K*, while for the relativistic liquid ^{3}He, it is $T_C = 4.5$ *K*. This shows that the relativistic corrections in liquid ^{3}He are relatively important, and the results are closer to the experimental data for the critical temperature ($T_C = 3.32$ *K*). Finally, we found that there is an overall agreement between our results and experimental results. Including the three-body cluster energy and spin polarization effects in the correlation function can improve the results. These issues can change the calculations to a more accurate one. However, the agreement between our results and the experimental data is rather good. Here, it should be noted that the extracted relativistic formalism of this work can be extended for the other dense correlated fermionic systems.

REFERENCES

[1] Dobbs, E. R., Helium Three, Oxford University Press, UK, **2000**, p. 3-30.

[2] Wilks, J., The Properties of Liquid and Solid Helium, Clarendon, Oxford, **1967**, p. 3-100.

[3] Baym, G.; Pethic, C. G., Landau Fermi-Liquid Theory, Wiley, New York, **1991**, p.10-50.

[4] Pines, D.; Nozierres, P., The Theory of Quantum Liquids, Vol. 1, Benjamin, New York, **1966**, p. 1-60.

[5] Kurten, K. E.; Ristig, M. L.; Clark, J. W., A correlated-basis-functions approach to realistic nuclear matter, *Nucl. Phys. A* **1979**, *317*, 87-115, DOI: 10.1016/0375-9474(79)90453-6.

[6] Wagner, L. K.; Ceperley, D. M., Discovering correlated fermions using quantum Monte Carlo, arXive: 1602.01344, **2016**, *& J. Casulleras, J. Boronat,* Progress in Monte Carlo Calculations of Fermi Systems: Normal Liquid ^{3}He, *Phys. Rev. Lett.,* **2000**, *84*, 3121-3125, DOI: http://dx.doi.org/10.1103/PhysRevLett.84.3121

[7] Krotscheck, E., Fermi-hypernetted chain theory for liquid 3He: A reassessment, *J. Low. Temp. Phys.* **2000**, *119*, 103-145, DOI: 10.1023/A:1004664619961.

[8] Clark, J. W.; Westhaus, P., Method of correlated basis functions, *Phys. Rev.* **1966**, *141*, 833-858, DOI: http://dx.doi.org/10.1103/PhysRev.141.833.

[9] Krotscheck, E.; Smith, R. A., Microscopic determination of the self-energy of ^{3}He, *Phys. Rev. B* **1983,** *27,* 4222-4236, DOI: http://dx.doi.org/10.1103/PhysRevB.27.4222.

[10] Gatica, S. M.; Hernandez, E. S.; Navarro, J., Spin-polarized ^{3}He in a density-functional frame, *Phys. Rev. B* **1998**, *58*, 12300-12306. DOI: http://dx.doi.org/10.1103/PhysRevB.58.12300.

[11] Stringari, S., Time dependent density functional

theory in quantum liquids, **1994**, arXiv:cond-mat/9411090.

[12] Manousakis, E., *et al*., Microscopic calculations for normal and polarized liquid ^{3}He, *Phys. Rev.* B **1983**, *26*, 3770-3782, DOI: http://dx.doi.org/10.1103/PhysRevB.28.3770.

[13] Dyugaev, A. M., Rough model of a quantum liquid, *Phys. Rev. Lett.* **1990**, *78*, 79-129, DOI: 10.1007/BF00682111.

[14] Bordbar, G. H.; Karimi, M. J., Variational Calculations for normal liquid ^{3}He at finite temperature using the spin-dependent correlation function, *Int. J. Mod. Phys. B* **2011**, *23*, 4359-4368, DOI: 10.1142/S0217979211059280.

[15] Bordbar, G. H.; Karimi, M. J.; Vahedi, J., LOCV Calculation for polarized liquid ^{3}He: The effect of three body cluster energy, *Int. J. Mod. Phys. B* **2009**, *25*, 2355-2363, DOI: 10.1142/S0217979211101260.

[16] Bordbar, G. H.; Karimi, M. J.; Poostfroush, A., Spin-spin correlation effect on the thermodynamic properties of the polarized liquid ^{3}He at finite temperature, *Eur. Phys. J. B* **2010**, *73*, 85-94 , DOI: 10.1140/epjb/e2009-00398-5.

[17] Jiang, L. J., *et al*., Self-consistent tensor effects on nuclear matter systems within a relativistic Hartree-Fock approach, *Phy. Rev. C* **2015**, *91*, 0258021-0258028, DOI: 10.1103/PhysRevC.91.025802.

[18] Li, A., *et al*., Nonrelativistic nucleon effective masses in nuclear matter: Brueckner-Hartree-Fock model versus relativistic Hartree-Fock model, *Phy. Rev. C* **2016**, *93*, 0158031-0158036, DOI: 10.1103/PhysRevC.93.015803.

[19] de Carvalho, C. A. A., Relativistic electron gas: A candidate for nature's left-handed materials, *Phys. Rev. D* **2016**, *93*, 1050051-1050058, DOI: 10.1103/PhysRevD.93.105005.

[20] Liu, Y.; Wu, J., Structure and thermo dynamic properties of relativistic electron gases, *Phys. Rev. E* **2014**, *90*, 0121411-0121416, DOI: 10.1103/PhysRevE.90.012141.

[21] Pyykko, P., Relativistic effects in chemistry: More common than you thought, *Annu. Rev. Phys. Chem.* **2012**, *63*, 45-64, DOI: 10.1146/annurev-physchem-032511-143755.

[22] Michauk, C.; Gauss, J., Perturbative treatment of scalar-relativistic effects in coupled-cluster calculations of equilibrium geometries and harmonic vibrational frequencies using analytic second-derivative techniques, *J. Chem. Phys.* **2007**, *127*, 0441061-0441068, DOI: http://dx.doi.org/10.1063/1.2751161.

[23] Boettcher, I., *et al*., Sarma phase in relativistic and non-relativistic systems, arXiv:1409.5232v1.

[24] Clark, J. W., Variational theory of nuclear matter, *Prog. Part. Nucl. Phys.* **1979**, *2*, 89-199, DOI: 10.1016/0146-6410(79)90004-8.

[25] Bordbar, G. H.; Modarres, M., LOCV calculation of nuclear matter with phenomenological two-nucleon interaction operators, *J. Phys. G: Nucl. Part. Phys.* **1997**, *23*, 1631-1646, DOI: http://dx.doi.org/10.1088/0954-3899/23/11/011.

[26] Fetter, A. L.; Walecka, J. D., Quantum theory of many-body system, New York, McGraw-Hill, **1971**, p. 40-100.

[27] Greywall, D. S., Specific heat of normal liquid ^{3}He, *Phys. Rev. B* **1983**, *27*, 2747-2767, DOI: http://dx.doi.org/10.1103/PhysRevB.27.2747.

[28] Fantoni, S.; Pandharipande, V. R.; Schmidt, K. E., Single-particle spectrum and specific heat of liquid ^{3}He, *Phys. Rev. Lett.* **1982**, *48*, 878-882, DOI: http://dx.doi.org/10.1103/PhysRevLett.48.878.

[29] Heller, P., Experimental investigations of critical phenomena, *Rep. Prog. Phys.* **1976**, *30*, 731, DOI: http://dx.doi.org/10.1088/0034-4885/30/2/307.